Author Manuscript

Title: Chiral Detection with Coordination Polymers

Authors: Shannon Thoonen; Carol Hua

To be cited as: 10.1002/asia.202100039

Link to VoR: https://doi.org/10.1002/asia.202100039

MINIREVIEW

Chiral Detection with Coordination Polymers

Shannon Thoonen,[a] Carol Hua*[a]

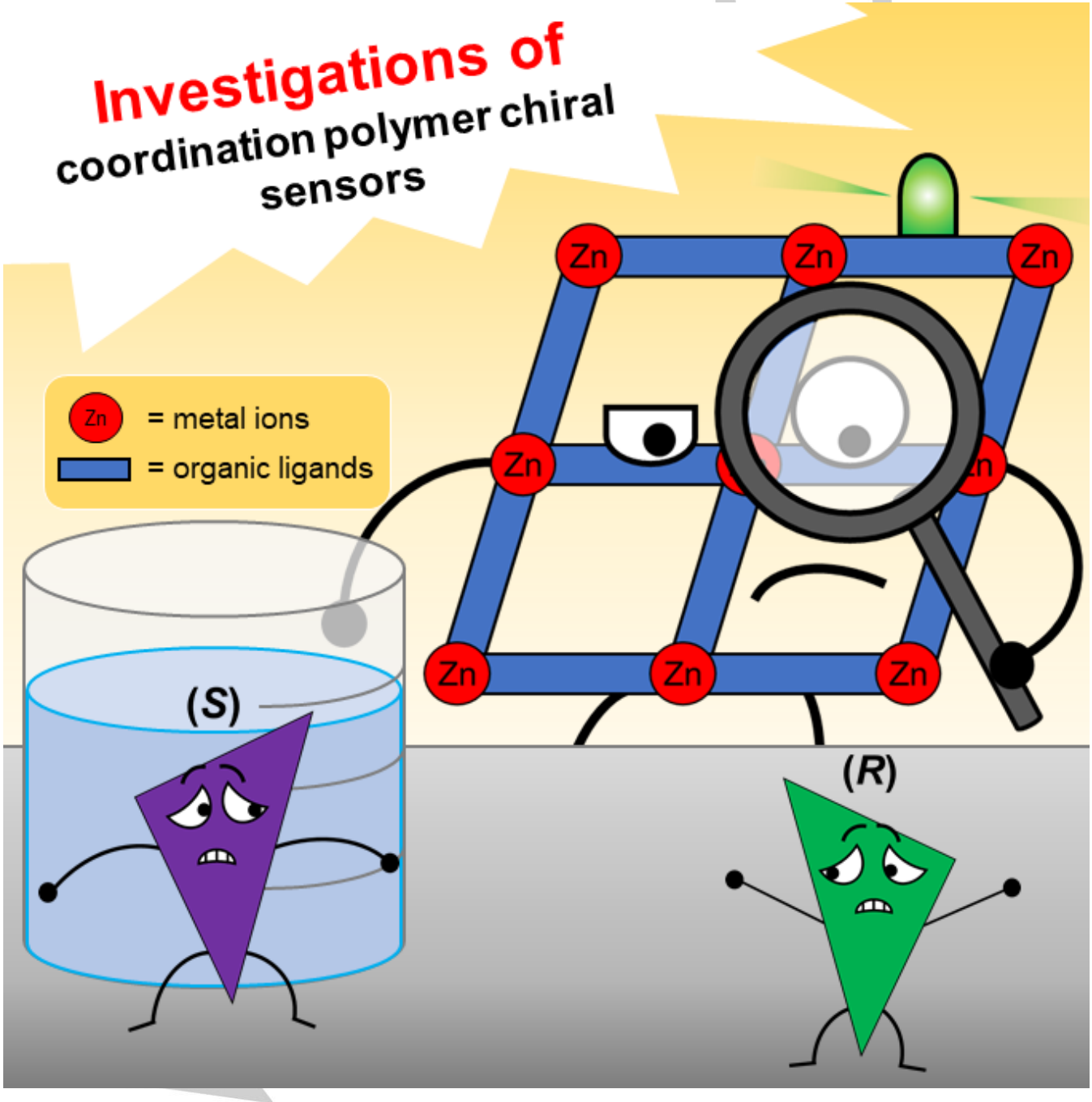

[a] S. Thoonen, Dr. C. Hua*
School of Chemistry
The University of Melbourne
Parkville, Victoria, 3010, Australia
E-mail: carol.hua@unimelb.edu.au

Abstract: Coordination polymers and metal-organic frameworks are prime candidates for general chemical sensing, but the use of these porous materials as chiral probes is still an emerging field. In the last decade, they have found application in a range of chiral analysis methods, including liquid- and gas-phase chromatography, circular dichroism spectroscopy, fluorescence sensing, and NMR spectroscopy. In this minireview, we examine recent works on coordination polymers as chiral sensors and their enantioselective host-guest chemistry, while highlighting their potential for application in different settings.

1. Introduction

Chirality is an integral aspect of the natural world. Nature has evolved over millions of years to incorporate chiral molecules, with even the fundamental building blocks of biology like DNA and proteins consisting of smaller chiral components.[1] These molecules exist as pairs of non-superimposable reflections of one another, called enantiomers, or optical isomers. Enantiomers are physically identical aside from their interactions with polarised light, and are chemically identical aside from their interactions with other chiral species.[2] As our biology is chiral at its core, this has reaching implications for natural systems.

This dichotomy is most apparent in the pharmaceutical industries. For example, the enantiomers of the anti-inflammatory drug, ibuprofen, differ in their effectiveness in the human body. (*S*)-ibuprofen is able to inhibit the cyclooxygenase enzyme, but (*R*)-ibuprofen is not, a difference which is caused by their respective complementarity with the shape of the enzyme's active site.[3] Similarly, while the D-enantiomer of penicillamine is effective at treating Wilson's disease and rheumatoid arthritis, L-penicillamine is toxic to humans.[4] Examples such as these incentivise manufacturers to differentiate and isolate the enantiomers of chiral compounds, leading to the development of chiral sensors.

Molecular chiral sensors include molecule-based probes,[5] as well as organic sensors,[6] but recent attention has been bestowed upon chiral coordination polymers (CPs) or metal-organic frameworks (MOFs). These frameworks, constructed from metal ions and organic bridges, are polymeric structures extending in 1D, 2D or 3D that can adopt chiral confirmations. CPs and MOFs have been demonstrated to be exceptionally tuneable for a multitude of applications, but most relevant is their potential to form porous networks.[7] Through host-guest chemistry, CPs may capture smaller ions or molecules within their channels and voids. When the host framework is chiral, and the guest is a chiral analyte, this generates diastereoisomers whose different physical properties can lead to enantiodifferentiation. CPs are ideal candidates for chiral sensing.

Interactions with a chiral analyte occur in various ways within CPs and MOFs, depending on the origin of chirality in the framework. Common strategies of generating a chiral structure are to simply include a chiral ligand;[8] to template the synthesis of the chiral network;[9] or to post-synthetically modify an existing achiral framework.[10] As such, there are diverse reasons behind the enantioselectivity of MOF-based chiral sensors. Functionalized chiral ligands can bind to analytes through covalent bonds, or non-covalent interactions such as hydrogen-bonding or π-π stacking. Helical structures can capture chiral guests through groove-binding, mimicking the enzymes that spiral around DNA strands. CPs and MOFs with chiral ions inserted in their channels can then undergo enantioselective ion exchange processes with a chiral compound. The range of host-guest interactions available involving CPs ensure they are adaptable to numerous chiral sensing techniques.

In this mini-review, we examine recent works in the emerging field of CPs and MOFs as chiral sensors, with emphasis on the sensing methods of chromatography, circular dichroism (CD) spectroscopy, fluorescent probing, and nuclear magnetic resonance (NMR) spectroscopy (**Figure 1**).

2. Chromatography

Chromatographic methods, involving the separation of enantiomers on a column, are perhaps the most easily applicable and extensively studied mode of chiral recognition with MOFs. Coordination polymers are used as chiral stationary phases (CSPs), interacting selectively with one enantiomer of a chiral analyte to increase its retention time in the column. This divergence in retention time generates two chromatographic peak, enabling the differentiation of enantiomers.

A distinction must be made here, between enantiodifferentiation – the recognition of enantiomers; and enantioseparation – the segregation of enantiomers. In all other sections of this review, the chiral sensing methods fall under the former category, but in the field of chromatography, the lines begin to blur. To effectively 'sense' chiral analytes with a chromatographic column, the pair of enantiomers must also be separated. These two processes go hand-in-hand.

Coordination polymers have been demonstrated as suitable CSPs in high-performance liquid chromatography (HPLC) and gas chromatography (GC), as well as the lesser-known field of capillary electrochromatography (CEC).

2.1. High-performance liquid chromatography (HPLC)

The most commonly utilized chromatographic technique is HPLC. In this method, analytes are separated over a column of CSPs by a liquid mobile phase, typically comprised of a mixture of organic solvents. The resolution of enantiomers can be affected by several factors, including the composition of the mobile phase and the solubility of the analyte.

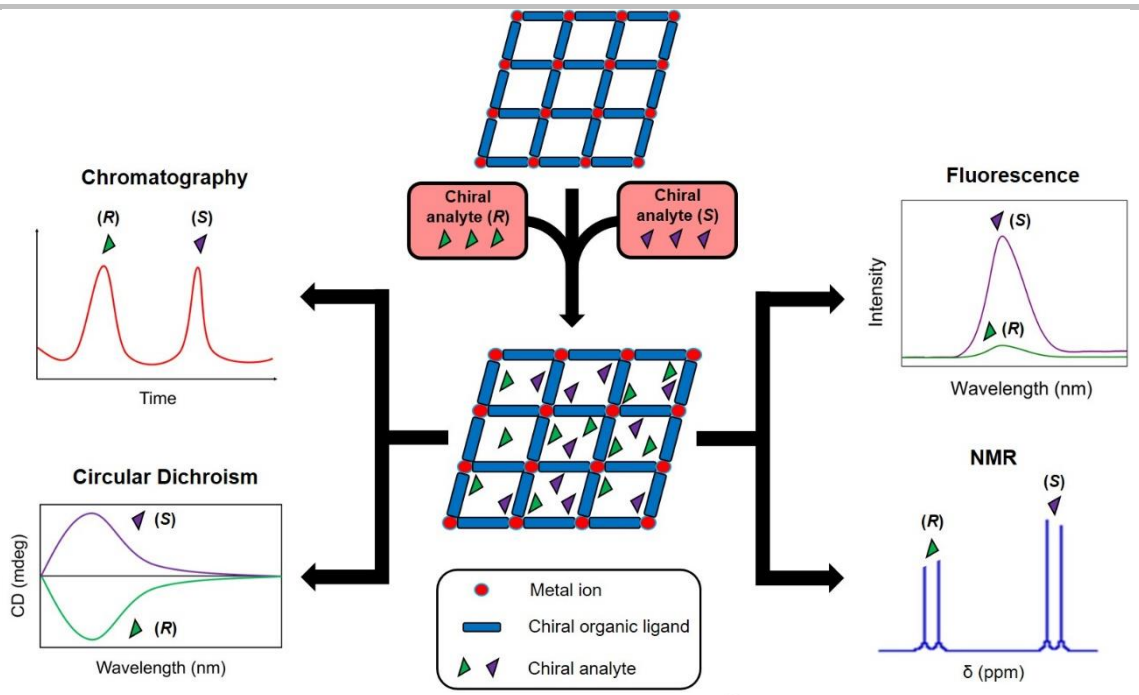

Figure 1. Chiral coordination polymers are novel chiral sensors when coupled with chromatography, CD spectroscopy, fluorescence sensing, and NMR spectroscopy.

Shannon Thoonen was born in Victoria, Australia and received his BSc at the University of Melbourne in 2019. Currently, he is an MSc student under Dr. Carol Hua, exploring the use of chiral coordination polymers as enantioselective fluorescence sensors.

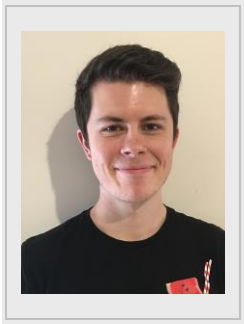

Carol Hua received her BSc in Advanced Science (Chemistry) from the University of New South Wales in 2011 and her PhD from the University of Sydney in 2016. She undertook two postdoctoral positions at the University of Limerick, Ireland and Northwestern University, USA before commencing her current position as a McKenzie Fellow at the University of Melbourne. Current research interests include the development of coordination polymers as chiral sensors.

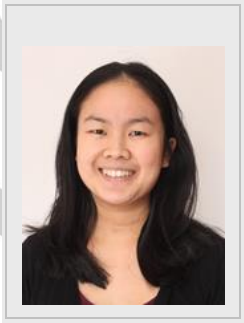

The first reported use of a chiral MOF as a HPLC stationary phase featured $[Zn_2(bdc)(L\text{-}lac)(dmf)] \cdot DMF$ (bdc = terephthalate).[11] The MOF enabled the separation of chiral sulfoxides, with complete separation achieved for methyl phenyl sulfoxide (PhSOMe) in a mixed DMF/CH_2Cl_2 mobile phase. Sulfoxides with additional electron-donating substituents received poorer enantioseparation. It was highlighted that greater complementarity between the size of the PhSOMe molecule and the inner pores of the MOF led to higher enantioselectivity.

An analogue of UMCM-1 $[Zn_4O(btb)_{4/3}(bdc)]$ (btb = benzene-1,3,5-tribenzoate) constructed from Bn-ChirBDC, which consists of terephthalic acid modified by the chiral auxiliary (*S*)-oxazolidinone, was assessed for chiral separation by HPLC.[12] The appendage of chiral auxiliary groups is well-known to generate predictable MOF structures, enabling a greater degree of control over the framework topology. The resulting MOF particles were too large for effective use as CSP, and so were manually crushed in a mortar-and-pestle prior to packing in a HPLC column and used for the separation of the enantiomers of 2-butanol and 1-phenylethanol. The enantioselectivity of the MOF-packed column was quantified as separation factors, which were 0.65 and 1.60, respectively.

This work highlights the importance of CSP particle size for its efficient performance in a HPLC column. An ideal HPLC stationary phase should have a particle size of less than 100 µm in diameter, within a narrow size distribution. MOF particles are often ground up before use in HPLC as they can be too large for efficient separation. Manual crushing, however, leads to irregular particle sizes and shapes, increasing the backpressure of the column and limiting reproducibility.[13] As an alternative, Yuan's group presented a Zn-based framework with the optimum particle size of 5-10 µm, eliminating the need for the mortar-and-pestle altogether.[14] The synthesis of chiral MOFs with appropriate size for enantioseparation by HPLC, such as through the use of modulators,[15] may be a strategy to consider in the future.

The framework $[(ZnLBr)(H_2O)]_n$ (HL = *N*-(4-pyridylmethyl)-L-leucine) possesses hexagonal windows and 1D helical channels, and was directly synthesized with 7 µm sized particles.[16] High resolution analysis with HPLC was attained for the racemic drug ibuprofen in under 6 minutes, in a hexane / isopropanol (95:5) mobile phase, with a separation factor of 2.40 (**Figure 2a**).

Additional chiral analytes included 1-phenylethylamine and 1-phenyl-1-propanol, where 1-phenylethylamine suffered a longer retention time due to the stronger interaction of the amine group with the framework. All the analytes had smaller kinetic diameters than the MOF's helical channels, so the authors attributed the enantioselectivity of the column to a 'molecular sieving effect', whereby both enantiomers can pass through the channels and differ only in the binding of their functional groups. To test this hypothesis, the enantiomers of benzoin were investigated – a larger molecule, but that one that fits within the boundaries of the MOF's channels. Baseline separation was still achieved for benzoin (**Figure 2d**). In contrast, racemates of ketoprofen and naproxen were unable to be separated, owing to their larger kinetic diameters. This proves the molecular sieving effect and confirms that the enantioselectivity of the MOF stems from its chiral channels.

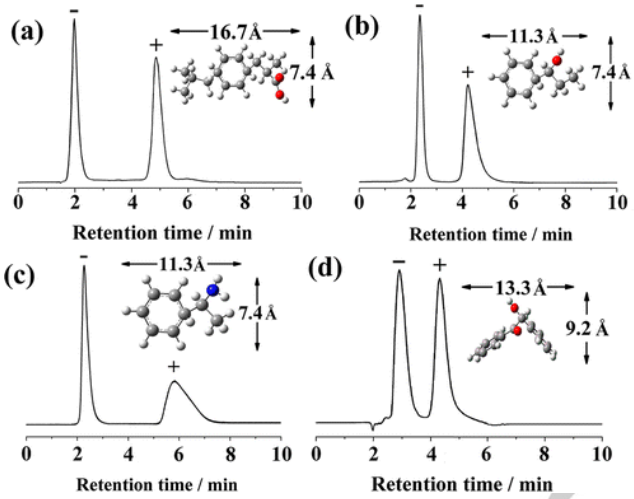

Figure 2. HPLC chromatograms showing the enantioseparation of racemates on a $[(ZnLBr)(H_2O)]_n$-packed column, with molecular models and kinetic diameters for each chiral analyte: (a) ibuprofen, (b) phenyl-1-propanol, (c) phenylethylamine, and (d) benzoin. Reproduced with permission.[16] Copyright 2014, American Chemical Society.

Conversely, the enantiomers of ibuprofen were also able to be resolved on the planar MOF $(Me_2NH_2)_2[Mn_4O(D\text{-cam})_4]\cdot 5H_2O$ (D-cam = D-camphoric acid), a framework which possesses channels smaller than the ibuprofen molecule.[17] As a consequence, the chiral sensing process relied solely upon noncovalent interactions along the surface of the framework.

An alternative approach is the combination of coordination polymers with silica gel to form MOF-silica composites, which provides a convenient way to generate more uniform particle sizes.[18,19] This was applied to the frameworks [Zn(BDA)(bpe)]·2DMA (H_2BDA = 1,1′-binaphthyl-2,2′-dihydroxy-5,5′-dicarboxylic acid, bpe = *trans*-bis(4-pyridyl)ethylene), and [Zn(BDA)(bpa)]·2DMA (bpa = *trans*-bis(4-pyridyl)ethane), which are based on derivatives of 1,1′-bi-2-naphthol, a popular organic molecule in enantioseparation chemistry. After slurry-packing these MOF-silica particles into HPLC columns, they were used to test various chiral sulfoxides, *sec*-alcohols, and flavanones, with separation factors up to 4.07 obtained for the enantiomer pairs. Of these frameworks, the MOFs with the highest resolving ability possessed the most appropriate steric fit for non-covalent interactions with the analyte. The homogenous particle size of the CSPs also boosted the separation efficiency of the column, and using silica gel to obtain these enhancements continues to be a viable strategy.[20]

All the studies listed have involved CSPs that are specific to one type of analyte or solvent condition, but others have set out to develop more versatile MOF-based CSPs. For example, TAMOF-1, or $[Cu(S\text{-TA})_2]\cdot n H_2O$ (*S*-TA = (*S*)-3-(1H-imidazol-5-yl)-2-(4H-1,2,4-triazol-4-yl)-propanoic acid), was used as a CSP for the HPLC separation of *trans*-2,3-diphenyloxirane enantiomers, as well as 1-phenylethanol, benzoin, and flavanone.[21] This column achieved baseline separation under a diverse range of eluent systems; as a result, the TAMOF-1 material was deemed a 'bifunctional CSP', since it performed sufficiently in both polar and nonpolar mobile phases.

Core-shell microspheres have also been developed for use as CSPs in HPLC enantioseparations, which build upon the previous ideas of MOF-silica composites.[22] These particles, synthesised by incorporating silica microspheres into the reaction mixture of histidine-modified ZIF-8, exhibited a uniform diameter of 5.5 µm, perfect for utilization as CSPs without any manual grinding. The resulting HPLC columns separated a total of eighteen racemates with separation factors up to 7.55, the highest yet documented. These excellent results are attributed to the regularity in particle shape and size afforded using composite microspheres. In addition, it was noted that exposed amino groups on the surface of the ZIF-8 microspheres enabled easy hydrogen-bonding with the analytes, enhancing separation efficiency.

2.2. Gas chromatography (GC)

GC has many fundamental advantages and disadvantages over the other chromatographic methods. GC can be used to achieve higher efficiency and sensitivity in the separation of enantiomers, at a faster rate, all without the need for solvents.[23] However, samples need to be thermally stable and volatile, leading to a lower diversity in the racemates able to be analysed.

The first example of a MOF used as the CSP in GC separations employed the helical framework $[Cu_2(sala)_2(H_2O)]_n$ (H_2sala) = *N*-(2-hydroxybenzyl)-L-alanine).[24] Upon heating, the MOF was desolvated and became the cross-linked structure $[Cu(sala)]_n$. This new framework showed excellent thermal stability and was ideal for GC experiments. With a thin (1 µm) coating of $[Cu(sala)]_n$, the fabricated column was able to separate several chiral analytes, including amino acids and racemic alcohols within a minute. Highest resolution was achieved for the enantiomers of valine and phenyl-succinic acid, with respective separation factors of 1.33 and 1.32.

The chiral diamond-type framework $InH(D\text{-cam})_2$ was subsequently used to fabricate a GC column with a 'dynamic coating method'.[25] This involved suspending the MOF in ethanol (2 mL) and flushing it through the capillary under gas pressure, leaving a wet 2 µm coating inside the wall. Several racemates, like 1-phenylethanol and limonene, were well-separated at a fast retention time, with respective separation factors of 1.44 and 1.35. $InH(D\text{-cam})_2$ has been combined with chiral cyclodextrins – which are popular CSPs in chromatography – and was found to enhance their coating properties.[26]

The cationic framework CMOM-3S, a variant of $[Co_2(man)_2(4,4'\text{-bpy})_3](NO_3)_2]$ (man = *S*-mandelate, 4,4´-bpy = 4,4´-bipyridine) incorporating triflate counteranions, was also used as a CSP in GC experiments.[27] The column coated with CMOM-3S enabled the separation of ten racemic alcohols and nitriles including 1-phenylethanol and 2-phenylbutyronitrile. In contrast to similar studies, this MOF also acted as a chiral crystalline sponge (CCS). This involved loading with a chiral guest and studying CMOM-3S via X-ray crystallography, which assisted in determining the absolute configuration of the analyte. This combination with CSS analysis meant that racemic identification through GC could be

carried out without a reference standard, and also confirmed that chiral recognition occured inside the pores of CMOM-3S.

In 2018, Kou *et al*. published a paper that was the first of its kind: a report of chiral MOFs synthesized by post-synthetic modification (PSM) for use as CSPs in chromatography.[28] Five frameworks were obtained from MIL-101-NH_2 by the covalent appendage of different chiral organic molecules to the amine groups in 2-aminoterephthalate. These post-synthetic modifiers were (*S*)-2-phenylpropionic acid, (*R*)-1,2-epoxyethylbenzene, diacetyl-L-tartaric anhydride, L-proline, and (1*S*)-10-camphorsulfonyl chloride. Each MOF-packed column performed differently for the separation of racemic alcohols and amines, but in all cases, the kinetic diameters of the chiral analytes were smaller than the pores of the MOFs. Accordingly, it is likely that chiral recognition took place within the channels of the frameworks. An advantage of using PSM in this way is to introduce chirality in pre-existing frameworks with well-defined pore sizes. This is especially useful when targeting a specific analyte, as knowledge of the cell dimensions eliminates the serendipitous nature of direct structural synthesis. The disadvantages of PSM, however, include framework degradation during the post-synthetic reaction conditions, potentially resulting in lower crystallinity or even collapse of the pores themselves. PSM also requires diffusion of the chiral substituent into the framework prior to modification, which can result in a lower incorporation of the chiral moiety.

2.3. Capillary electrochromatography (CEC)

Though not as popular amongst chemists, CEC has found some use in recent years as a novel enantioseparation technique with MOF-based CSPs. This analysis method marries the established selectivity of liquid chromatography with the extra separation efficiency of electrophoresis, eluting analytes in a mobile phase driven by electroosmotic flow (EOF). By applying a voltage, racemates can be separated without backpressure, with lower consumption of organic solvents, and with lessened impact on the environment.[29,30] The dependence of the process on charged particles and EOF requires careful choice of a pH buffer.

The earliest report of chiral MOF-based CEC uses the self-penetrating $[Zn_2(D\text{-cam})_2(4,4'\text{-bpy})]_n$.[31] The column was constructed using a dynamic coating method and used to separate flavanone and praziquantel. While the enantioselectivity results is predominately influenced by the steric fit of the analytes in the MOF channels, the π-π between pyridine rings in the MOF and benzyl groups on the analytes also play a role.

Pan and co-workers posited in 2018 that since DNA molecules have been proven to be naturally effective CSPs, artificial materials emulating the double-helix structure of DNA would be well-suited to enantioseparations.[32] As such, they employed the double helical zeolitic framework JLU-Liu23, which consists of two separate interpenetrated structures: $[Cu_4I_4(dabco)_2]_n$ (dabco = 1,4-diazabicy-clo[2.2.2]-octane); and $[Cu_2(bbimb)]_n$, (bbimb = 1,3-bis(2-benzimidazol)-benzene). Although these components are achiral, the resulting double-helix was definitely chiral, allowing enantioseparations be to carried out in a CEC column. A range of racemic neurotransmitters; epinephrine, isoprenaline, synephrine and terbutaline, were separated with a 10 mM borate buffer / methanol (85:15) mixed mobile phase and a 15 kV applied voltage. All enantioselectivity was attributed to 'groove binding', or intercalative interactions, between the analytes and the specific helices in the structure, much like DNA.

As recently as 2020, a monolithic capillary was built with a Zn-based zeolitic imidazole MOF named Pepsin-ZIF-8.[33] In a rare example of chirality bestowed by post-synthetic modification, ZIF-8 was self-assembled layer-by-layer on the surface of a poly(GMA-co-EDMA) monolithic column and only later became chiral after covalently linking with pepsin molecules. With a 20 mM ammonium acetate buffer and an applied voltage of 15 kV, the monolithic capillary enabled good separation of hydroxychloroquine, chloroquine, hydroxyzine, and amlodipine. Compared to a previously tested Pepsin-poly(GMA-co-EDMA) monolithic column, the chiral resolution of Pepsin-ZIF-8 was high, demonstrating the applicability of coordination polymers to CEC separations.

Despite the popularity of chromatography – be it HPLC, GC, or CEC – the interactions between host coordination polymers and chiral analytes in this enantioseparation technique are still vague. All the reports listed in this section note that the mechanisms of chiral recognition in CSPs are still not entirely understood – although, some do give experimental evidence suggesting that interactions take place within the pores of the studied MOFs. Most common is the description of a suitable 'steric fit' in the framework channels, in which enantioselectivity arises based on which enantiomer fits most snugly inside the pores of the coordination polymers. It is this steric selection that allows chiral molecules to be filtered through the MOF in chromatographic columns.

3. Optical sensing

3.1. Circular dichroism (CD) spectroscopy

CD spectroscopy, involving the opposite interaction of enantiomers with circularly polarized light, is a technique most often used in the characterization of coordination polymers, not sensing. However, the enantiomeric composition of a sample can be determined by capturing a chiral guest with a host MOF and monitoring the change in the CD spectrum, typically in the UV/vis range. CD spectroscopy also allows the absolute configuration of a probed analyte to be visually identified, an advantage that the other sensing techniques in this review do not possess.

CD spectroscopy was used to analyse surface-anchored chiral MOFs after incorporation of chiral guest compounds.[34] The framework used for chiral recognition, $[Cu_2(D\text{-cam})_2(dabco)]$, was grown layer-by-layer on OH-terminal quartz glass, then loaded with the D/L-enantiomers of ethyl-lactate. By comparing the CD spectra of the empty MOF and the loaded MOF, then calculating the difference, the contribution of each enantiomer to the CD signal could be determined. Specifically, the relative amount of each enantiomer present in the sample could be quantified by integrating the areas under the signal curves. For instance, Gu and co-workers obtained an ee value of 28% for one racemate based on the intrinsic chirality of the host framework, which implies a composition of 64% ethyl-D-lactate and 36% ethyl-L-lactate.

The framework $[Zn(RR\text{-PCCHC})_2]$ (RR-PCCHC = (1*R*, 2*R*)-2-(pyridine-4-ylcarbamoyl) cyclohexanecarboxylate) was designed as a MOF-based CD sensor and exhibited a right-handed double-helix structure reminiscent of DNA.[35] It was expected that the mechanism of chiral amino acid recognition would be groove binding in the same way as DNA, which was supported by computational studies. While eight amino acids were investigated, only aspartic acid was used to construct a calibration curve. It was found that polar R-groups of amino acids led to better chiral recognition than non-polar varieties, undoubtedly due to the hydrogen-bonding of groove binding. Aspartic acid achieved an enantioselectivity factor of ~1.35 based on the ratio of recognition efficiencies, which is in contrast to the non-polar phenylalanine, with an enantioselectivity factor of only ~1.11. The CD signal of

the MOF decreased in intensity with increasing amounts of aspartic acid, which was more pronounced for the L-enantiomer.

The use of CD for sensing is relatively rare in MOFs; however, limited reports exist from the Wang group.[36,37] The CD sensing of a zeolitic imidazolate framework synthesised by the solvent-assisted linker exchange (SALE) of ZIF-78 was investigated with proline as the analyte.[38] Racemic mixtures of different enantiomeric ratios (e.g. 1:1, 2:1, 3:1, 1:3, 1:2, 1:1) produced either positive or negative CD signals in the MOF, with varying intensity. Interestingly, when the MOF was added to a 1:1 sample (i.e. a racemic mixture), a negative Cotton effect was observed. This suggested that the concentration of L-proline in the mixture decreased more than D-proline, indicating the framework's preference for the L-enantiomer.

In a particularly important paper showcasing the power of CD for chiral sensing, Zhang *et al*. used the zeolitic framework MOZ-51, or $[N(CH_3CH_2)_4]_2[Zn_4(5\text{-mtz})_6(D\text{-cam})_2]$ · 2DMF (5-mtz = 5-methyltetrazole).[39] Amino acid derivates were included in the framework through ion exchange with the achiral tetraethyl ammonium cation. The CD signals of MOZ-51 decreased upon loading with the D/L-enantiomers of alanine methyl ester, represented by D-A^+ and L-A^+, respectively (**Figure 3**). The intensity of the signal decreased more for the L-enantiomer, indicating a faster ion exchange between $[N(CH_3CH_2)_4]^+$ and L-A^+ than $[N(CH_3CH_2)_4]^+$ and D-A^+. The CD spectrum of a racemic camphoric acid solution displayed no signal – however, the addition of MOZ-51 to the solution resulted in a negative signal. The negative signal represents an excess of D-A^+ in solution and confirms a faster ion exchange process for L-A^+ , which allowed a calibration curve to be constructed for the CD signal intensity *vs*. the ee of the sample.

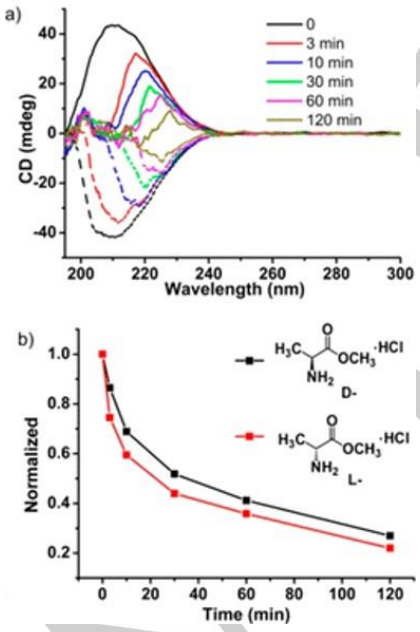

Figure 3. (a) CD spectra of L-alanine methyl ester (represented by solid lines) and D-alanine methyl ester (represented by dashed lines) after immersion with MOZ-51. (b) Decrease in normalized CD intensity upon the incorporation of D- and L-alanine methyl ester over time. Adapted with permission.[39] Copyright 2020, American Chemical Society.

3.2. Fluorescence sensing

The use of enantioselective fluorescent probes is by far the simplest and most rapid method of chiral recognition presented in this review. The technique operates in a similar fashion to CD spectroscopy, but without the requirement of circularly polarized light, and can be conducted with a standard fluorimeter. When a MOF traps a chiral guest, there may be a corresponding fluorescent response: either enhancement or quenching of the emission intensity. This response differs between the enantiomers of the analyte, allowing enantiodifferentiation to occur.

A pioneering paper by Wanderley *et al*. provided a blueprint for these works.[40] The fluorescent framework $[Cd_2(L)(H_2O)_2]$ · 6.5DMF · 3EtOH (L-H_4 = (*R*)-2,2′-dihydroxy-1,1′-binaphthyl-4,4′,6,6′-tetrakis(4-benzoic acid)) was used as an enantioselective sensor for chiral amino alcohols, namely 2-amino-1-propanol, 2-amino-2-phenylethanol, 2-amino-3-phenylpropanol, and 2-amino-3-methyl-1-butanol. The MOF was found to form hydrogen-bonds with the chiral analytes, specifically in the fluorescent BINOL core of the ligands. The fluorescence of the framework was quenched upon binding with all four amino alcohols, but the extent of this quenching differed between enantiomers. As such, the enantioselectivity of the MOF sensor was able to be calculated as a quenching ratio (QR) of the Stern-Volmer constants for each enantiomer. The highest enantioselectivity was achieved for 2-amino-3-methyl-1-butanol, with a QR of 3.12 (**Figure 4b**). The construction of a calibration curve for the enantiomeric excess (ee) of 2-amino-3-methyl-1-butanol allowed the enantiomeric composition of samples to be rapidly determined using fluorescence measurements (**Figure 4c**).

The chiral framework $[Zn_8L_4I_8]$·4MeOH·4H_2O (H_2L^0 = *N*,*N*-bis(3-*tert*-butyl-5-(4-pyridyl)salicylidene)-1,2-diaminocyclohexane), was tested as a chiral fluorescent sensor with five chiral saccharides: D-sorbitol, D-maltose, D-glucose, D-galactose, and D-fructose.[41] The MOF possesses helical channels adorned with amino functional groups for guest adsorption. Fluorescent enhancement was observed upon binding with D-sorbitol, but more so for the (*S*)-enantiomer of the MOF. The enantioselectivity of the sensing method was then expressed as a ratio of association constants, with the highest value of 4.943 for D-sorbitol. Later, the chiral sensor was studied in the solid-state, which involved exposing the (*R*)-enantiomer of the MOF to the vapours of 1-cyclohexylethylamine. The emission maximum of the framework shifted from 530 nm to 565 nm and was enhanced by both enantiomers of the analyte, but to a greater extent with the (*R*)-enantiomer. The ratio of enhancements was taken as an enantioselectivity factor of 3.60.

One study showcases a rare example of symmetry-breaking crystallization of achiral precursors, which produced the framework [Cd(L)(4,4′-bpy)] · DMA · 5H_2O (H_2L = 4,4′-((naphthalene-1,4-dicarbonyl)bis(azanediyl)) dibenzoic acid).[42] The MOF adopted an (*S*)-conformation, suggesting it was more amenable to crystallization than the opposite conformation. This chiral framework showed fluorescence quenching upon adsorption of penicillamine, particularly for D-penicillamine, with a QR of 3.6.

Alternatively, one can post-synthetically modify an achiral framework to not only induce chirality in the system but enhance its fluorescent properties as well.[43] One example involved exchange of the dimethyl ammonium cations in $[(CH_3)_2NH_2]_{1/2}[Zn_2(\text{adenine})(TATAB)O_{1/4}]$ · 6.5DMF · 4H_2O (H_3TATAB = 4,4′,4″-*s*-triazine-1,3,5-triyltri-*p*-aminobenzoic acid)

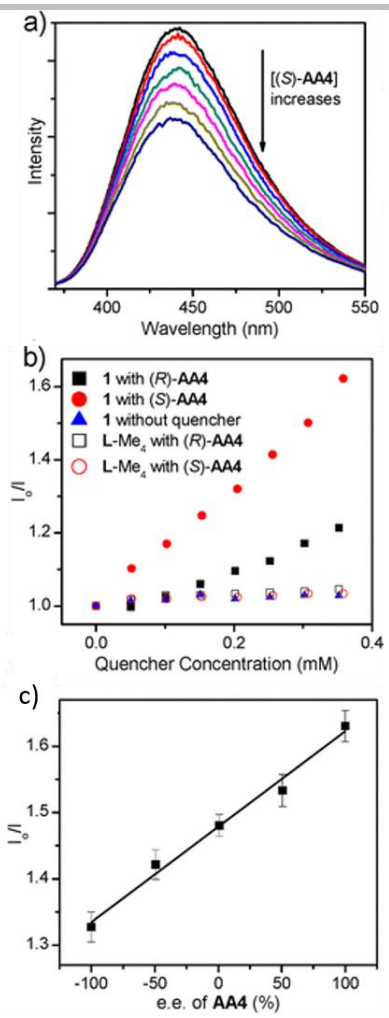

Figure 4. (a) Fluorescence spectra of $[Cd_2(L)(H_2O)_2]\cdot 6.5DMF\cdot 3EtOH$ with (*S*)-2-amino-3-methyl-1-butanol (AA4) added in increments. (b) Quenching of the framework with increasing concentration of the analyte. (c) Calibration plot of quenching *vs*. the ee of the analyte. Adapted with permission.[40] Copyright 2012, American Chemical Society.

for *N*-benzyl quininium and insertion of Tb^{3+} ions (**Figure 5**).[44] The result was a bifunctional MOF: by taking the ratio of luminescence responses from the dual centres, the ee values of chiral analytes can be directly quantified. The authors tested their MOF on the epimers cinchonine and cinchonidine, the former of which was favourably adsorbed by the framework. Enantioselectivity was driven by hydrogen-bonding and π-π stacking interactions, leading to a QR of 1.4. Later, an achiral version of the MOF lacking the *N*-benzyl quininium cation was quenched by both epimers, but without any enantioselectivity, proving the cation's role in chiral recognition.

Compared to the vast library of studies into chromatographic enantioseparation, the optical methods of chiral sensing have been less explored. Chiral MOFs built for CD spectroscopy and fluorescence sensing are in their infancy and have a huge potential for growth. Enantioselectivity using optical techniques has been attributed mainly to hydrogen-bonding and π-π stacking, though the steric fit of the analyte within the chiral channels of a MOF certainly still plays a role. It is primarily the non-covalent interactions that form diastereomeric complexes in the material,

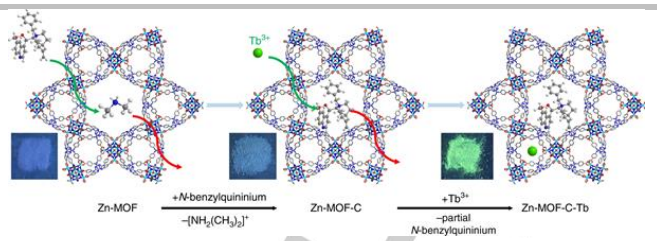

Figure 5. The post-synthetic ion exchange in $[(CH_3)_2NH_2]_{1/2}[Zn_2(adenine)(TATAB)O_{1/4}]\cdot 6.5DMF\cdot 4H_2O$, generating chirality and supplementing the fluorescent properties in the framework. Atoms are represented as follows: carbon (grey), hydrogen (white), oxygen (red), zinc (turquoise), terbium (green). Reproduced under the Creative Commons Attribution 4.0 International License with credit.[44]

leading to optical responses from the framework. Steric fit is not as important here as it is in the molecular sieving effect of chromatography.

4. NMR spectroscopy

Of all the chiral sensing methods utilising MOFs and CPs, the application of NMR spectroscopy is the most recent. MOFs are employed in this area as chiral shift reagents, where the formation of two non-equivalent diastereomeric complexes with the enantiomers of a chiral analyte results in different physical properties. The resulting NMR spectrum will exhibit two signals with different chemical shifts, allowing each enantiomer to be identified.

The first example of chiral elucidation with MOFs in solid-state NMR utilized chiral analogues of the UMCM-1 framework, namely *i*Pr-Chir-UMCM-1 (*i*Pr = isopropyl) and Bn-Chir-UMCM-1 (Bn = benzene).[45] These MOFs were loaded with the enantiomers of 1-phenyl-2,2,2-trifluoroethanol (TFPE), then analysed using ^{13}C cross-polarization magic-angle spinning (CP MAS) NMR spectroscopy. The ^{13}C NMR signals of the chiral side groups showed different chemical shifts 0.1-0.4 ppm apart depending on which enantiomer of TFPE was loaded.

The previously studied Zn-based DUT-32, comprised of the 4,4′,4″-[benzene-1,3,5-triyl*tris*(carbonylamino)]trisbenzoate ligand, was used as an achiral basis for building a MOF for NMR sensing.[46] After modification with a BOC-protected derivative of proline, *N*-(*tert*-butoxycarbonyl)-L-proline, the chiral framework DUT-32-NHProBoc was formed. This MOF was also tested with TFPE and analysed by ^{13}C CP MAS NMR. Upon loading with TFPE, the NMR signals of the proline-derived ligand were shifted, with a difference of 0.1-0.6 ppm obtained. Also of note was the narrowing of the NMR peak shape for the (*S*)-loaded sample, which was absent for the (*R*)-loaded sample.

Later, the chiral *trans*-1,2-diaminocyclohexane was grafted onto the enantiopure framework, *R*- or *S*-Mg_2(dobpdc) (dobpdc = 4,4′-dioxidobiphenyl-3,3′-dicarboxylate), to form an enantioselective sensor.[47] The chiral MOF was able to adsorb CO_2, which reacted with the diamine molecules in the structure and generated ammonium carbamate chains. Subsequently, further CO_2 adsorption occurred in an enantioselective manner. However, most interesting were the ammonium carbamate chains, which exhibited a different chemical shift in the ^{13}C CP MAS NMR spectrum based on which enantiomer of Mg_2(dobpdc) was originally used. This chemical shift difference was ~3 ppm, the largest value reported to date.

In a combination of the techniques from the previous two studies, our group grafted a series of BOC-protected amino acids (alanine, valine and proline) onto *S*-Mg_2(dobpdc).[48] By observing the ^{13}C CP MAS NMR signals for specific carbon atoms in the dobpdc^{4-} ligand, the D/L-enantiomers of each BOC amino acid derivative could be distinguished. Chemical shift differences up to 0.6 ppm were observed between enantiomers, with the largest difference obtained for BOC-alanine (**Figure 6**). This result was attributed to the smaller size of the alanine side chain, with the methyl group affording less steric bulk and allowing stronger non-covalent interactions within the pores of the MOF. Further analysis was undertaken on unprotected amino acid samples following thermal deprotection of the BOC groups, with even larger chemical shift differences obtained up to 1.3 ppm. It was the absence of the large BOC group that led to this larger enantioselectivity, enabling stronger interactions between the pure amino acid and the MOF which boosted chiral recognition ability. Of particular note was the ability of *S*-Mg_2(dobpdc) to distinguish between the enantiomers of BOC-alanine and alanine from a racemic mixture, which was not able to be achieved in previous reports on the use of MOFs and CPs for chiral elucidation.

The use of MOFs and CPs as chiral shift reagents in NMR is still new, with limited examples. Chiral analytes have been restricted to a handful of amino acid and TFPE derivatives, yielding small chemical shift differences.[49] It is only in the last few years that these values have been extended beyond 1.0 ppm, but this increase in enantioselectivity gives hope for the future of the sensing field's applicability. The increased ability of chemists to design MOFs and CPs with highly complementary pores for the encapsulation of the chiral analyte and use of lanthanide metal ions will enable larger chemical shift differences to be obtained.

5. Summary and outlook

The use of CPs and MOFs as chiral sensors is relatively new, but recent studies have laid the groundwork for a diverse range of enantioselective sensors. For all sensing techniques, a strong interaction between the chiral analyte and the CP or MOF is required to yield high levels of chiral discrimination. The types of non-covalent interactions that have been highlighted in this review include the complementary fit of an analyte within a framework's voids, and intermolecular interactions such as hydrogen bonding, π-π interactions, and groove binding.

The scope of these sensors has been limited to certain analytes, with it being rare that a framework can differentiate between the enantiomers of multiple chiral compounds. Similarly, the degree of enantioselectivity achieved varies by framework. In chromatography, enantioseparation factors up to 7.55 have been attained with MOFs. Fluorescence sensors constructed from CPs have achieved enantioselectivity factors – represented by quenching ratios – up to 3.60. NMR sensors have obtained chemical shift differences up to 3.0 ppm, though most of these values reside below the 1.0 ppm mark. These enantioselectivity factors are modest, but they are promising, because they have increased over time since the initial concept of the field. As more studies are released into this emerging area, the enantioselectivity factors attainable can only climb.

However, to increase the enantiodifferentiation efficiency of these frameworks, the underlying chiral mechanisms need to be better understood. The reported ways that CPs and MOFs facilitate chiral discrimination are still vague. As the number of chiral MOF-based sensors grows, a fundamental study of this nature will be easier to undertake, and provide an effective roadmap for the targeted synthesis of CPs and MOFs for enantioselective sensing. For example, these mechanistic studies might aid the production of more versatile MOF sensors, able to distinguish between the enantiomers of multiple analytes. Enantioselectivity factors will rise when the interactions between framework and guest are focused and deliberate. The construction of all chiral sensors will benefit from a closer look at CPs and MOFs.

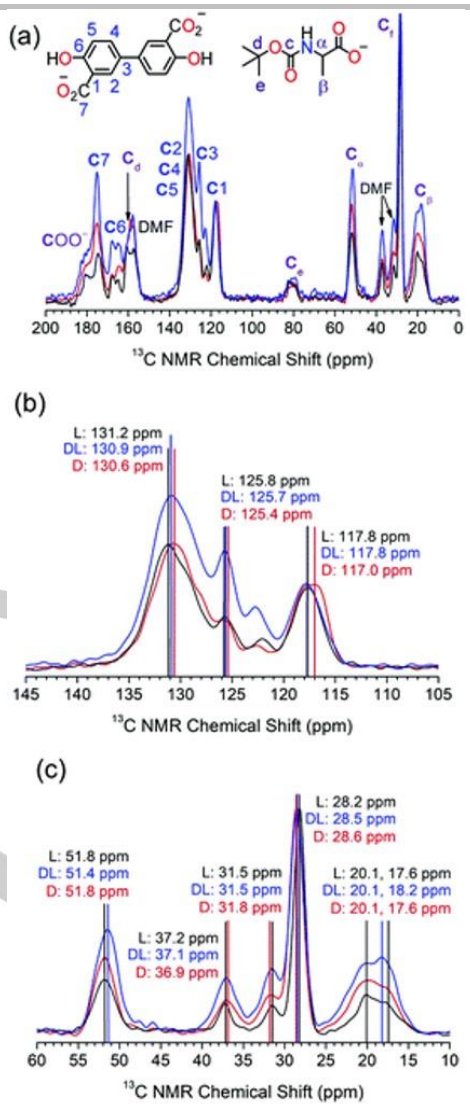

Figure 6. ^{13}C CP MAS NMR spectra of *S*-Mg_2(dobpdc) appended with BOC-L-alanine (black), BOC-D-alanine (red), and BOC-DL-alanine (blue), showing (a) the full spectrum, (b) magnified section between 145-105 ppm, and (c) magnified section between 60-10 ppm. Adapted with permission from the Royal Society of Chemistry.[48]

Acknowledgements

C.H. gratefully acknowledges the University of Melbourne for a McKenzie Fellowship.

Keywords: Chirality • Metal-organic frameworks • Coordination polymers • Sensors • Enantioselectivity

Table 1. A list of chiral MOFs and their respective sensing types, as well as the enantioselectivity factors achieved for given chiral analytes.

Framework	Sensing type	Analytes used	Enantioselectivity factor[a]	Ref.
$[Zn_2(bdc)(L\text{-}lac)(dmf)]\cdot DMF$	HPLC	PhSOMe *p*-MePhSOMe *p*-BrPhSOMe PhSO*i*Pr	---	[11]
$[Zn_4O(btb)_{4/3}(bdc)]$ with Bn-ChirBDC	HPLC	2-butanol 1-phenyl-ethanol	SF = 0.65 SF = 1.60	[12]
$[(ZnLBr)(H_2O)]_n$	HPLC	Ibuprofen	SF = 2.40	[16]
$(Me_2NH_2)_2[Mn_4O(D\text{-}cam)_4]\cdot 5H_2O$	HPLC	Ibuprofen	SF = 6.48	[17]
[Zn(BDA)(bpe)]·2DMA-silica composite	HPLC	16 sulfoxides 11 *sec*-alcohols 5 flavanones	SF ≤ 1.84 SF ≤ 4.07 SF ≤ 3.10	[18]
[Zn(BDA)(bpa)]·2DMA-silica composite	HPLC	16 sulfoxides 11 *sec*-alcohols 5 flavanones	SF ≤ 3.03 SF ≤ 1.93 SF ≤ 1.90	[18]
$[Cu(S\text{-}TA)_2]\cdot n H_2O$	HPLC	*trans*-2,3-diphenyloxirane Furoin 1-phenylethan-1-ol Flavanone Benzoin 1-(1-naphthyl)-ethanol Benzoin Praziquantel 1,1′-bi-2-naphthol Hydrobenzoin *trans*-stilbene oxide Warfarin Naproxen Flurbiprofen Zopiclone Salbutamol Ibuprofen Alprenolol Metoprolol Ketoprofen Citronellal Camphor Alanine Leucine Valine Isoleucine Proline 2-methyl-1-butanol 1-phenyl-1,2-ethandiol Phenyl-succinic acid 1-phenyl-ethanol Citronellal 1-phenyl-1,2-ethandiol 1-phenyl-ethanol 2-amino-1-butanol Limonene Methionine Proline	SF ≤ 7.24 SF = 1.57 SF ≤ 1.72 SF ≤ 2.84 SF = 1.54 SF = 7.13 SF = 5.70 SF = 3.29 SF = 3.96 SF = 2.35 SF = 1.15 SF = 2.38 SF = 7.55 SF = 1.20 SF = 6.74 SF = 2.26 SF = 1.85 SF = 1.33 SF = 2.62 SF = 1.77 SF = 1.26 SF = 1.02 SF = 1.31 SF = 1.12 SF = 1.33 SF = 1.30 SF = 1.17 SF = 1.01 SF = 1.28 SF = 1.32 SF = 1.29 SF = 1.13 SF = 1.17 SF = 1.44 SF = 1.25 SF = 1.35 SF = 1.10 SF = 1.32	[21] [22] [24] [25]
D-His-ZIF-8@SiO_2	HPLC			[22]
$[Cu(sala)]_n$	GC			[24]
$InH(D\text{-}cam)_2$	GC			[25]
CMOM-3S	GC	1-phenylethanol 1-phenyl-1-propanol 1-phenyl-2-propanol α-vinylbenzyl alcohol 2-phenylpropanenitrile 1-phenyl-1-butanol 1-phenyl-1-pentanol 1-phenyl-2-butanol α-cyclopropylbenzyl alcohol 2-phenylbutyronitrile	---	[27]

MIL-101(Al)-*S*-2-Ppa	GC	2-methyl-2,4-pentanediol 1,2-pentanediol Citronellal	---	[28]
MIL-101(Al)-*R*-Epo	GC	2-butanol 1-heptyn-3-ol Citronellal	---	[28]
MIL-101(Al)-(+)-Ac-L-Ta	GC	1-amino-2-propanol 2-amino-1-butanol 1,2-pentanediol	---	[28]
MIL-101(Al)-L-Pro	GC	Mandelonitrile 1-phenylethylamine Methyl-2-chloroproprionate	---	[28]
$[Zn_2(D\text{-}cam)_2(4,4'\text{-}bpy)]_n$	CEC	Flavanone Praziquantel	---	[31]
JLU-Liu23	CEC	Epinephrine Synephrine Isoprenaline Terbutaline	---	[32]
Pepsin-ZIF-8	CEC	Hydroxychloroquine Chloroquine Hydroxyzine Nefopam Clenbuterol Amlodipine	---	[33]
$[Cu_2(D\text{-}cam)_2(dabco)]$	CD	Ethyl-lactate	---	[34]
$[Zn(RR\text{-}PCCHC)_2]$	CD	Tyrosine Histidine Phenylalanine Aspartic acid Threonine Proline Alanine Valine	---	[35]
S-ZIF-78h	CD	Proline	---	[38]
$[N(CH_3CH_2)_4]_2[Zn_4(5\text{-}mtz)_6(D\text{-}cam)_2]\cdot 2DMF$	CD	Alanine methyl ester hydrochloride	---	[39]
$[Cd_2(L)(H_2O)_2]\cdot 6.5DMF\cdot 3EtOH$	Fluorescence	2-amino-1-propanol 2-amino-2-phenylethanol 2-amino-3-phenylpropanol 2-amino-3-methyl-1-butanol	QR = 1.25 QR = 1.17 QR = 1.39 QR = 3.12	[40]
$[Zn_8L_4I_8]\cdot 4MeOH\cdot 4H_2O$	Fluorescence	D-sorbitol D-maltose D-glucose D-galactose D-fructose 1-cyclohexylethylamine	EF = 4.49 EF = 3.49 EF = 4.38 EF = 2.48 EF = 4.18 EF = 3.60	[41]
$[Cd(L)(4,4'\text{-}bpy)]\cdot DMA\cdot 5H_2O$	Fluorescence	Penicillamine	QR = 3.60	[42]
$[(CH_3)_2NH_2]_{1/2}[Zn_2(adenine)(TATAB)O_{1/4}]\cdot 6.5DMF\cdot 4H_2O$ (with *N*-benzyl quininium and Tb^{3+})	Fluorescence	Cinchonine/ cinchonidine	QR = 1.40	[44]
*i*Pr-Chir-UMCM-1	NMR	TFPE	≤ 0.4 ppm difference	[45]
DUT-32-NHProBoc	NMR	TFPE	≤ 0.6 ppm difference	[46]
$Mg_2(dobpdc)$	NMR	*trans*-1,2-diaminocyclohexane	3 ppm difference	[47]
S-$Mg_2(dobpdc)$	NMR	BOC-alanine BOC-valine BOC-proline Alanine Valine Proline	≤ 1.3 ppm difference	[48]

[a] Enantioselectivity factors are cited based on ratios given in the literature (e.g. separation factors, quenching ratios, etc.).

[1] S. Mason, *Trends Pharmacol. Sci.* **1986**, *7*, 20–23.

[2] D. S. Bradshaw, J. M. Leeder, M. M. Coles, D. L. Andrews, *Chem. Phys. Lett.* **2015**, *626*, 106–110.

[3] A. M. Evans, *Clin. Rheumatol.* **2001**, *20*, 9–14.

[4] I. A. Jaffe, K. Altman, P. Merryman, *J. Clin. Invest.* **1964**, *43*, 1869–1873.

[5] Y. Y. Zhu, X. D. Wu, S. X. Gu, L. Pu, *J. Am. Chem. Soc.* **2019**, *141*, 175–181.

[6] X. Wu, X. Han, Q. Xu, Y. Liu, C. Yuan, S. Yang, Y. Liu, J. Jiang, Y. Cui, *J. Am. Chem. Soc.* **2019**, *141*, 7081–7089.

[7] H. C. Zhou, J. R. Long, O. M. Yaghi, *Chem. Rev.* **2012**, *112*, 673–674.

[8] W. X. Guo, Y. Y. Wang, X. L. Hu, Q. Yue, E. Q. Gao, *Cryst. Growth Des.* **2020**, *20*, 5072–5085.

[9] L. Ma, C. Abney, W. Lin, *Chem. Soc. Rev.* **2009**, *38*, 1248–1256.

[10] J. Zhao, H. Li, Y. Han, R. Li, X. Ding, X. Feng, B. Wang, *J. Mater. Chem. A* **2015**, *3*, 12145–12148.

[11] A. L. Nuzhdin, D. N. Dybtsev, K. P. Bryliakov, E. P. Talsi, V. P. Fedin, *J. Am. Chem. Soc.* **2007**, *129*, 12958–12959.

[12] M. Padmanaban, P. Müller, C. Lieder, K. Gedrich, R. Grünker, V. Bon, I. Senkovska, S. Baumgärtner, S. Opelt, S. Paasch, E. Brunner, F. Glorius, E. Klemm, S. Kaskel, *Chem. Commun.* **2011**, *47*, 12089.

[13] M. Zhang, Z.-J. Pu, X.-L. Chen, X.-L. Gong, A.-X. Zhu, L.-M. Yuan, *Chem. Commun.* **2013**, *49*, 5201.

[14] M. Zhang, X.-D. Xue, J.-H. Zhang, S.-M. Xie, Y. Zhang, L.-M. Yuan, *Anal. Methods* **2014**, *6*, 341–346.

[15] A. Ranft, S. B. Betzler, F. Haase, B. V Lotsch, *CrystEngComm* **2013**, *15*, 9296.

[16] X. Kuang, Y. Ma, H. Su, J. Zhang, Y.-B. Dong, B. Tang, *Anal. Chem.* **2014**, *86*, 1277–1281.

[17] R. Hailili, L. Wang, J. Qv, R. Yao, X.-M. Zhang, H. Liu, *Inorg. Chem.* **2015**, *54*, 3713–3715.

[18] K. Tanaka, N. Hotta, S. Nagase, K. Yoza, *New J. Chem.* **2016**, *40*, 4891–4894.

[19] K. Tanaka, T. Muraoka, Y. Otubo, H. Takahashi, A. Ohnishi, *RSC Adv.* **2016**, *6*, 21293–21301.

[20] P. Zhang, L. Wang, J.-H. Zhang, Y.-J. He, Q. Li, L. Luo, M. Zhang, L.-M. Yuan, *J. Liq. Chromatogr. Relat. Technol.* **2018**, *41*, 903–909.

[21] M. N. Corella-Ochoa, J. B. Tapia, H. N. Rubin, V. Lillo, J. González-Cobos, J. L. Núñez-Rico, S. R. Balestra, N. Almora-Barrios, M. Lledós, A. Güell-Bara, J. Cabezas-Giménez, E. C. Escudero-Adán, A. Vidal-Ferran, S. Calero, M. Reynolds, C. Martí-Gastaldo, J. R. Galán-Mascarós, *J. Am. Chem. Soc.* **2019**, *141*, 14306–14316.

[22] Y. Yu, N. Xu, J. Zhang, B. Wang, S. Xie, L. Yuan, *ACS Appl. Mater. Interfaces* **2020**, *12*, 16903–16911.

[23] S.-M. Xie, X.-H. Zhang, Z.-J. Zhang, M. Zhang, J. Jia, L.-M. Yuan, *Anal. Bioanal. Chem.* **2013**, *405*, 3407–3412.

[24] S.-M. Xie, Z.-J. Zhang, Z.-Y. Wang, L.-M. Yuan, *J. Am. Chem. Soc.* **2011**, *133*, 11892–11895.

[25] S.-M. Xie, X.-H. Zhang, Z.-J. Zhang, L.-M. Yuan, *Anal. Lett.* **2013**, *46*, 753–763.

[26] J. Yang, S.-M. Xie, H. Liu, J. Zhang, L. Yuan, *Chromatographia* **2015**, *78*, 557–564.

[27] S. Y. Zhang, C. X. Yang, W. Shi, X. P. Yan, P. Cheng, L. Wojtas, M. J. Zaworotko, *Chem* **2017**, *3*, 281–289.

[28] W.-T. Kou, C.-X. Yang, X.-P. Yan, *J. Mater. Chem. A* **2018**, *6*, 17861–17866.

[29] M. M. Dittmann, G. P. Rozing, in *J. Chromatogr. A*, Elsevier B.V., **1996**, pp. 63–74.

[30] K. D. Altria, *J. Chromatogr. A* **1999**, *856*, 443–463.

[31] Z.-X. Fei, M. Zhang, J.-H. Zhang, L.-M. Yuan, *Anal. Chim. Acta* **2014**, *830*, 49–55.

[32] C. Pan, W. Lv, X. Niu, G. Wang, H. Chen, X. Chen, *J. Chromatogr. A* **2018**, *1541*, 31–38.

[33] W. Ding, T. Yu, Y. Du, X. Sun, Z. Feng, S. Zhao, X. Ma, M. Ma, C. Chen, *Microchim. Acta* **2020**, *187*, 51.

[34] Z.-G. Gu, J. Bürck, A. Bihlmeier, J. Liu, O. Shekhah, P. G. Weidler, C. Azucena, Z. Wang, S. Heissler, H. Gliemann, W. Klopper, A. S. Ulrich, C. Wöll, *Chem. - A Eur. J.* **2014**, *20*, 9879–9882.

[35] Y.-W. Zhao, Y. Wang, X.-M. Zhang, *ACS Appl. Mater. Interfaces* **2017**, *9*, 20991–20999.

[36] F. Wang, Y.-H. Tang, J. Zhang, *Inorg. Chem.* **2015**, *54*, 11064–11066.

[37] M.-Y. Li, F. Wang, Z.-G. Gu, J. Zhang, *RSC Adv.* **2017**, *7*, 4872–4875.

[38] C. Zhuo, F. Wang, J. Zhang, *CrystEngComm* **2018**, *20*, 5925–5928.

[39] M. Y. Li, F. Wang, J. Zhang, *Cryst. Growth Des.* **2020**, *20*, 5644–5647.

[40] M. M. Wanderley, C. Wang, C.-D. Wu, W. Lin, *J. Am. Chem. Soc.* **2012**, *134*, 9050–9053.

[41] J. Dong, Y. Zhou, F. Zhang, Y. Cui, *Chem. - A Eur. J.* **2014**, *20*, 6455–6461.

[42] Q. Zhang, M. Lei, F. Kong, Y. Yang, *Chem. Commun.* **2018**, *54*, 10901–10904.

[43] T.-Y. Liu, X.-L. Qu, B. Yan, *J. Mater. Chem. C* **2020**, *8*, 14579–14586.

[44] Z. Han, K. Wang, Y. Guo, W. Chen, J. Zhang, X. Zhang, G. Siligardi, S. Yang, Z. Zhou, P. Sun, W. Shi, P. Cheng, *Nat. Commun.* **2019**, *10*, 5117.

[45] H. C. Hoffmann, S. Paasch, P. Müller, I. Senkovska, M. Padmanaban, F. Glorius, S. Kaskel, E. Brunner, *Chem. Commun.* **2012**, *48*, 10484.

[46] C. Kutzscher, H. C. Hoffmann, S. Krause, U. Stoeck, I. Senkovska, E. Brunner, S. Kaskel, *Inorg. Chem.* **2015**, *54*, 1003–1009.

[47] J. D. Martell, L. B. Porter-Zasada, A. C. Forse, R. L. Siegelman, M. I. Gonzalez, J. Oktawiec, T. Runčevski, J. Xu, M. Srebro-Hooper, P. J. Milner, K. A. Colwell, J. Autschbach, J. A. Reimer, J. R. Long, *J. Am. Chem. Soc.* **2017**, *139*, 16000–16012.

[48] H. M. Tay, A. Rawal, C. Hua, *Chem. Commun.* **2020**, *56*, 14829–14832.

[49] X. Ma, Y. Zhang, Y. Gao, X. Li, C. Wang, H. Yuan, A. Yu, S. Zhang, Y. Cui, *Chem. Commun.* **2020**, *56*, 1034–1037.

Entry for the Table of Contents

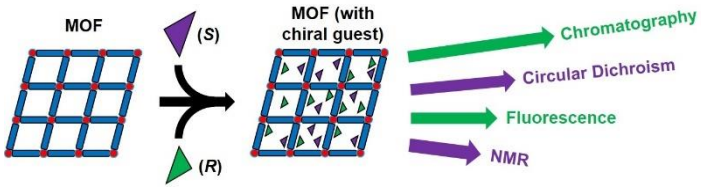

Chiral coordination polymers and metal-organic frameworks are showing increasing potential as chiral sensors. These porous materials undertake enantioselective host/guest chemistry and are able to be linked with chromatography, circular dichroism, fluorescence probing, and NMR spectroscopy to differentiate between the enantiomers of chiral compounds.